SIZING OF CRACKS EMBEDDED IN SUB-CLADDING USING ULTRASONIC SYNTHETIC APERTURE FOCUSING TECHNIQUE (SAFT)

Sony Baby[1], T. Balasubramanian[1], R. J. Pardikar[2], K.V. Rajkumar[3], T. Jayakumar[3] and Baldev Raj[3]

[1]Department of Physics, National Institute of Technology, Tiruchirappalli, Tamil Nadu, India, [2]NDTL, Bharat Heavy Electricals Limited, Tiruchirappalli, Tamil Nadu, India, [3]Indira Gandhi Centre for Atomic Research, Kalpakkam, Tamil Nadu, India

Abstract: This paper deals with the experimental work carried out to demonstrate the feasibility of ultrasonic Synthetic Aperture Focusing Technique (SAFT) to obtain improved detection and sizing of vertical/inclined (10° and 15°) simulated cracks underneath different claddings. Crack heights ranging from 1.68mm to 19.04mm underneath stainless steel, Inconel and ferritic steel cladding could be sized with an accuracy of ±0.1 to ±0.3 mm. The problems encountered in TOFD with regard to sizing of near surface cracks was successfully overcome by SAFT. Mis-oriented (inclined) defects embedded below the cladding suffer added disadvantage due to loss of reflected energy due to mis-orientation. Using SAFT even these defects could be sized accurately.

Introduction: Pressure vessels heat exchangers and many other components used in many applications such as nuclear reactors, petrochemical, power plants and paper mills are typically fabricated from thick carbon steel covered with austenitic stainless steel cladding. The purpose of the clad is to protect the carbon steel from the environment in the vessel; typically, the clad is not considered a structural part of the vessel. Clad is applied by welding using either an automated or manual process. These clads pose problem for the ultrasonic inspection during the routine inservice inspection. Inspection procedures based on NDE play an important role in structural integrity assessment and this involves the knowledge of the defects present in the structure in the areas particularly subjected to stresses induced by the pressurized thermal shock (PTS). These defects include sub-clad defects of the planar type generally perpendicular to the surface such as under clad cracks; weld cracks, lack of fusion and defects in the cladding. The most commonly used NDE method for these applications is ultrasonic testing. Evaluation of the acceptability of detected flaws according to ASME Section XI requires measurement of the depth of the flaw extending into the base metal. Accurate crack depth or size determination and cracks growth monitoring are essential for safe operation of critical components in industrial plants [(1)]. To obtain accurate defect sizes using conventional ultrasonic NDT equipment, considerable skill is required because; there are many factors, which affect the accuracy and sizing ability of the ultrasonic inspection. Two main factors that affect ultrasonic inspection of cladded components are: (a) the effect of clad, and (b) the beam spread of ultrasonic beam at longer range. The presence of a welded cladding layer particularly austenitic type, seriously affects the ultrasonic inspection due to its coarse grained anisotropic structure and the surface irregularities this leading to beam skewing, scattering and mode conversion of ultrasonic waves. The heavy scattering of ultrasonic waves in coarse grain structure of the clad results in poor signal to noise (S/N) ratio, in turn resulting in poor detection sensitivity. This problem is minimized to some extent by utilization of longitudinal wave angle beam probes, instead of shear wave angle beam probes, with compromise on lower detection sensitivity for the same frequency. The other factor, which predominates especially at long ranges, is the probe beam spread [(2)]. The larger the beam spread, the greater is the inaccuracy in defect sizing. In order to overcome the above limitations i.e. to get better detection sensitivity, and sizing ultrasonic SAFT can be employed. The higher S/N ratio achieved by spatial averaging which is inherent in SAFT is effectively used to precisely size defects embedded in clad. The sizing by SAFT is more accurate which can be employed by the fracture mechanics engineer for integrity assessment. Beam spread which is highly disadvantageous in the case of conventional UT is effectively used to get focused beam characteristics by employing the beam steering algorithm. Hence better detection sensitivity is obtained and thus results in reliable detection and better sizing of defects even in presence of highly scattering type of clad.

Ultrasonic SAFT based studies were made on different carbon steel blocks having artificial surface breaking cracks (machined slit), which were subsequently embedded by cladding with different clad materials are discussed in this paper. The studies have been confined only to simulated cracks. The steel test blocks used for the study contained 0.5mm wide vertical/inclined slits (10° and 15° inclination) of various heights ranging from 1.68mm to 19.04mm underneath the Stainless Steel, Inconel and Ferritic steel cladding. These studies have been carried out to determine the through thickness height of vertical/inclined simulated cracks underneath cladding by using SAFT. To ascertain the actual dimensions of the defects after their embedment by cladding, radiography has been used. Sizing of the defects were also carried out on the same blocks using Time of Flight Diffraction (TOFD) in a separate study have been compared with that of the results obtained by SAFT and radiography. The study could clearly bring out the effectiveness of SAFT for detection of near surface defects. This study also shows the better sizing accuracy of SAFT, also promises in accurately sizing the height of defect that are smaller than 2mm even in the presence of highly attenuating stainless steel clad overlay material of 18.2 mm. This paper makes an assessment of the usefulness of ultrasonic based SAFT inspection for detection and evaluation of underclad defects in cladded blocks.

Principle of SAFT: The synthetic aperture method is based on the concept of collecting data from a scanned transducer and then processing that data, so as to simulate a larger transducer with much better resolution and S/N ratio. The argument is based on the idea that the more often the discontinuity is seen by the transducer, the more information that can be gathered about it. The more the information that is known, the more precisely the discontinuity can be located. Thus, a highly divergent beam is used to keep a discontinuity in view over as large an aperture as possible. The principle of SAFT is schematically shown in Figure 1 [(3)]. When the transducer is located directly above the discontinuity, the time delay to receive the defect echo is minimum and as the transducer moves away from this position, the time delay increases in a non-linear fashion. The curve defined by tracing the peak amplitude (in each aperture element) as the transducer moves parallel to the surface is a function of the speed of the sound in the material and the geometry of the transducer and the target.

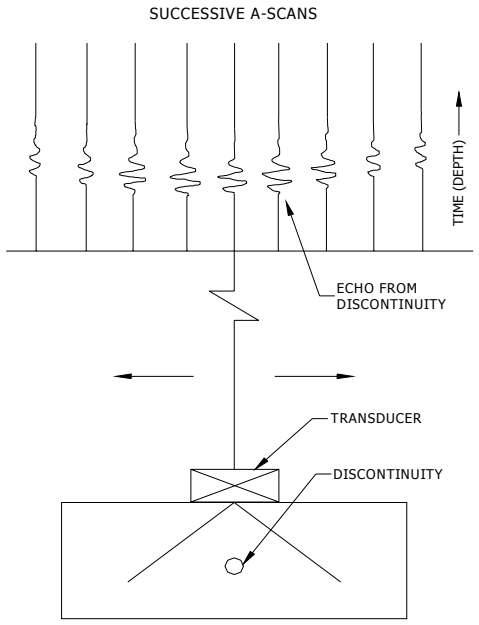

Figure 1: Data Acquisitions of A-scans in SAFT

Synthetic aperture processing involves collection of aperture elements to be processed as a unit to introduce a time shift to each individual A-scans, to sum these individual aperture elements point by point across their length and then to place the result at the center of the chosen aperture. The process is shown schematically in Figure 2 (the aperture is chosen to be of seven aperture elements wide). If the aperture is centered over the target, as in the case of Figure 2, then the shift and sum operation will produce a strong signal (constructive interference). If the aperture is located off center of the target as in Figure 3, then the shift and sum operation will produce a weak signal (destructive interference) [4]. Reflections coming from defect are constructively added and other signals such as grain noise and electronic noise are destructively summed, resulting in good S/N ratio for the defect [5]. Since simultaneous focusing is obtained along the entire depth of the test specimen, better accuracy is expected [6].

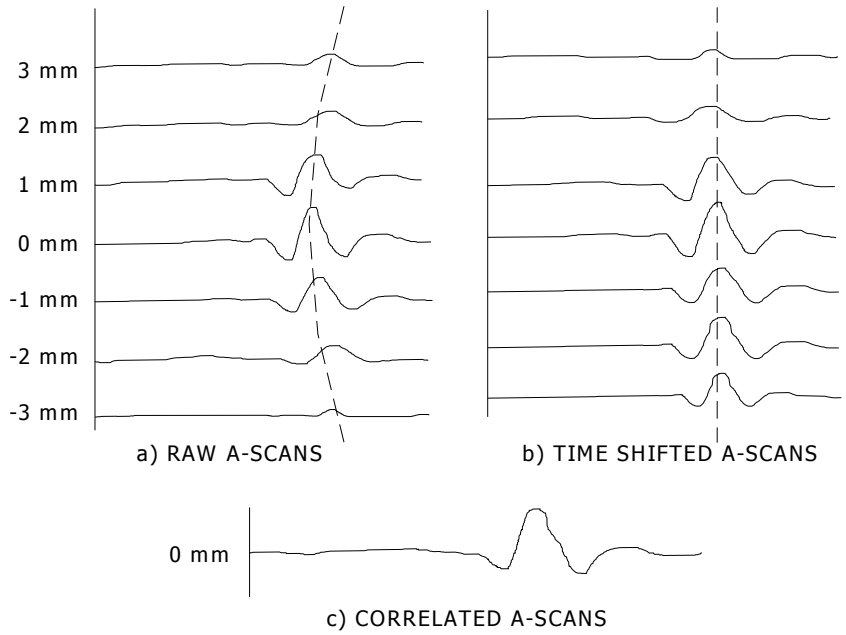

Figure 2. Showing constructive interference

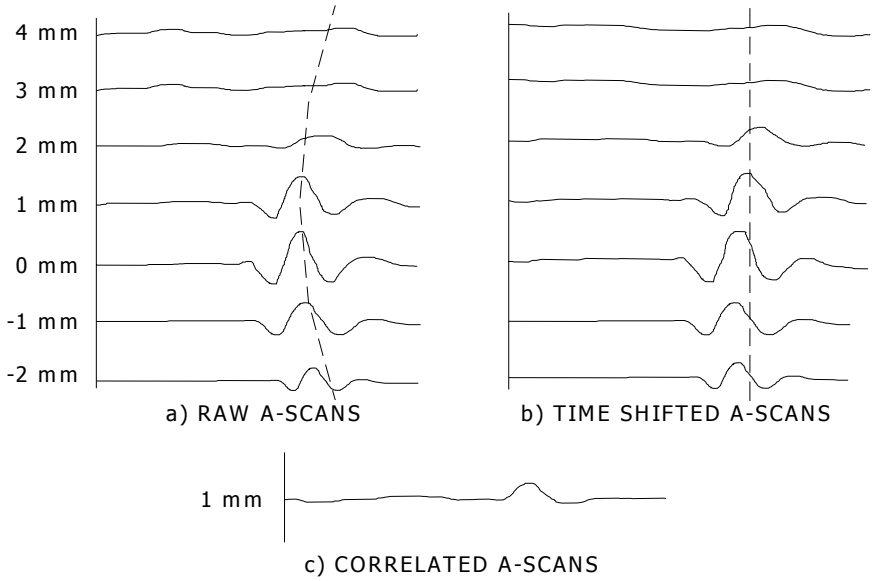

Figure 3: Showing destructive interference

The axial resolution of the SAFT is equal to the pulse length and not related to the aperture. Sizing of the crack is independent upon the selected probe step distance. SAFT

relies less on amplitude information but more on time-of-flight information. Loss of amplitude influences only the S/N ratio in the image. The data acquisition in SAFT is based upon the complete high-frequency ultrasonic signal, without time gate or amplitude threshold. Due to the time corrected signal averaging capability of SAFT, signals which are buried within the noise can rise be brought to amplitudes above the noise [7].

Experimental Study: Artificial surface breaking defects were made on carbon steel test blocks by machined slits, which were subsequently embedded by cladding with different clad materials. These slits simulated the embedded cracks and the study was confined only on these simulated cracks. The carbon steel test blocks used for the study contained 0.5mm wide vertical/inclined cracks (10°and15°inclination) of various heights ranging from 1.68mm to 19.04mm underneath the Stainless Steel, Inconel and Ferritic steel cladding.

Cladding of test blocks for embedment of cracks: Following procedures were used for embedding the cracks:

Stainless Steel cladding on carbon steel blocks: The first layer of the cladding was done very carefully using SMAW process, with E 309, φ 4mm electrode, current: 130-140Amps, voltage: 22-24V and preheating to 423 K . However for subsequent layers, the electrodes used were E 347 without preheat. The interpass temperature was maintained at maximum 393 K.

Ferritic steel cladding on carbon steel blocks: The cladding was done using SMAW process, with E 7018, φ 4mm electrodes, by preheating to 423 K. The tempering bead was necessary to reduce heat affected zone (HAZ).

Inconel cladding on carbon steel blocks: The first layer of the cladding was done very carefully using SMAW process, with UTP 068 HH, φ 4mm electrode, current: 130-140Amps, voltage: 22-24V and preheating to 423 K. However for subsequent layers, no preheating was required. The inter-pass temperature was maintained at maximum 393 K.

The cladding was done for all the eight blocks on both the surfaces. Precautions were taken to reduce the dilution to the minimum. However, the original crack height got altered due to dilution. The final dimensions of the slit height after completing the cladding were measured from radiography and are given in Tables 1, 2 and 3. Radiography was carried out from the side face of the block. The actual dimensions of the block and the location and size of the simulated cracks (slits) are shown in Figure 4. Machining was done to even out the surface roughness so as to carry out the ultrasonic inspection under similar condition of all the blocks.

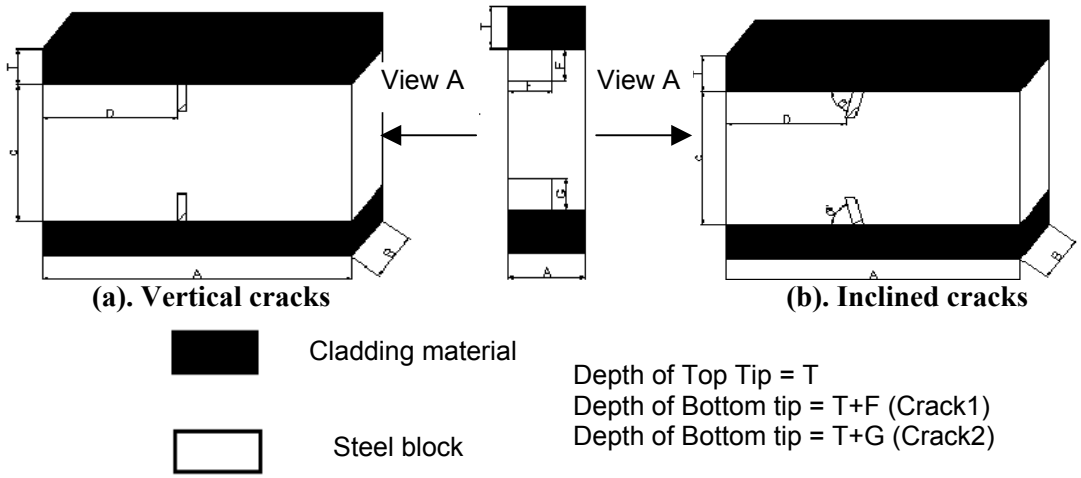

Figure 4: Schematic diagram of the steel blocks showing the location and size of the sub-cladded vertical and inclined simulated cracks (slits)

Table 1: Dimensional detail of test blocks after embedment of the simulated vertical cracks (slits) by cladding

DIM / BL No.	Cladding material	A	B	C	D	E	F	G
BL.1	Inconel	248	39.8	36.08	124	20	4.56	-
BL.2	SS	247.5	39.8	46.78	128.75	25	8.44	1.88
BL.3	Ferritic	200	48.5	51.84	100	30	18.02	1.68
BL.4	Ferritic	250	39.10	68.08	125	25	13.72	3.51

Table 2: Dimensional details of test blocks after embedment of the simulated inclined cracks (slits) by cladding

DIM / BL No.	Cladding material	A	B	C	D	E	F	G*	θ^0
BL.5	SS	231.7	37	81.27	115.85	25	5.01	1.90	15
BL.6	Inconel	130.3	37.4	89.11	115.15	20	9.22	6.80	15
BL.7	Ferritic	225.3	41.3	141.50	112.65	25	14.30	11.93	10
BL.8	Ferritic	300.6	41	133.89	150.3	25	19.04	17.31	10

Note: All the dimensions are given in mm

* A - length, B - width, C - thickness, D - distance of the crack from one end of the block, E - length of the crack, F and G - height of the surface breaking cracks.

Table 3: Location details and actual dimensions of the simulated cracks (slits) after embedment by cladding

Cladding material	Block No.	Top surface cladding	Crack-1			Crack- 2			
			Depth of top tip	Depth of bottom tip	Crack height	Bottom surface cladding	Depth of top tip	Depth of bottom tip	Crack height
Vertical Cracks									
Inconel	01.	5.44	5.44	10	4.56	-	-	-	-
SS	02.	6.19	6.19	14.63	8.44	14.32	30.58	32.46	1.88
Ferritic	03.	7.24	7.24	25.26	18.02	9.58	40.58	42.26	1.68
Ferritic	04.	21.23	21.23	34.95	13.72	19.52	45.05	48.56	3.51
Inclined Cracks									
SS	05.	18.26	18.26	23.27	5.01	8.97	70.4	72.3	1.90
Inconel	06.	19.77	19.77	28.99	9.22	18.67	63.64	70.44	6.80
Ferritic	07.	10.87	10.87	25.17	14.30	19.39	110.18	122.11	11.93
Ferritic	08.	12.23	12.23	31.27	19.04	24.02	92.56	109.87	17.31

Figure 5: Experimental set up of SAFT

Carried out the measurements by using SAFT to determine the through thickness height of vertical/inclined simulated cracks underneath the cladding. Longitudinal angle beam probe of 45°- 4MHz was used for the study. A PC based version of the SAFT in the time domain was used. Automated scan and digital recording of ultrasonic data was carried out with Line SAFT Manufactured by M/s IZFP, Germany. The hardware consists of a modified ultrasonic unit USD 10 by M/s. Krautkramer, a computer, a FIFO DMA-Interface and a scanner with scanner control unit. At every step the RF signals were digitized at 30 MHz. The stepper movement was controlled by intelligent manipulator system. This is a modular positioning control system, which is particularly suitable for the automated manipulator of sensor-systems in the field of nondestructive testing. The SAFT reconstruction was performed off line. The experimental set up of SAFT is shown in Figure 5.

Table 4: Estimation of through thickness height of simulated cracks (slits)

Actual crack height by Radiography (mm)	Measured Crack height by SAFT (mm)	Measured Crack height by TOFD (mm)
Vertical Cracks		
1.68	1.6	2.76*
1.88	1.7	2.59*
3.51	3.5	3.52
4.56	4.5	4.40
8.44	8.4	7.87
13.72	13.6	13.70
18.02	17.9	18.20
Inclined Cracks		
1.90	1.8	1.93
5.01	5.0	5.20
6.80	7.1	6.64
9.22	9.1	9.35
11.93	12.0	11.50
14.30	13.9	14.08
17.31	16.9	16.68
19.04	19.4	19.04

*Measurement taken from opposite side

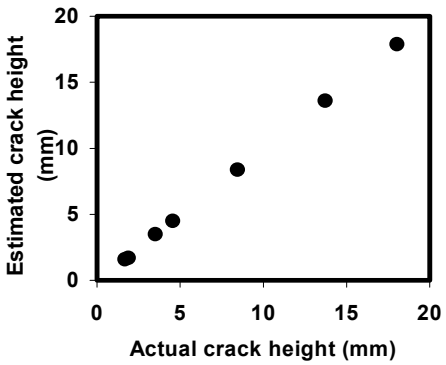

Figure 6: Estimation of through thickness height for vertical cracks

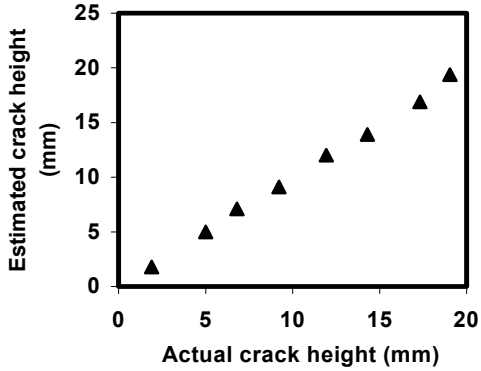

Figure 7: Estimation of through thickness height for inclined cracks

Results and Discussion: In conventional ultrasonic testing, sizing accuracy gets affected by the poor S/N ratio obtained in the presence of cladding. Inclined cracks pose further problems due to lower reflected energy due to their unfavorable orientation. Moreover in the conventional manual ultrasonic testing, the non uniformity of couplant at a few locations and the skill of the person performing ultrasonic testing play a major role in the defect sizing accuracy [(4)]. Automatic scanning using the intelligent manipulator and the spatial averaging

inherent to SAFT were used to overcome such problems. The experimental observations with respect to through thickness height of the simulated cracks obtained by radiography, SAFT and TOFD are shown in Table 4. The TOFD measurements carried out on the same blocks, in a separate study have been used for comparison [8]. Comparing the results of SAFT and TOFD, it was found that defects smaller than 2mm in height have been oversized by TOFD. For crack height more than 2mm, the accuracy of sizing by both the techniques is more close to the actual crack height obtained by radiography. Figures 6 and 7 gives the graphical representation of the actual crack height obtained by radiography Vs estimated height of the cracks using SAFT, for vertical and inclined slits respectively. Figure 8 shows the actual SAFT images of a few of the vertical and inclined cracks.

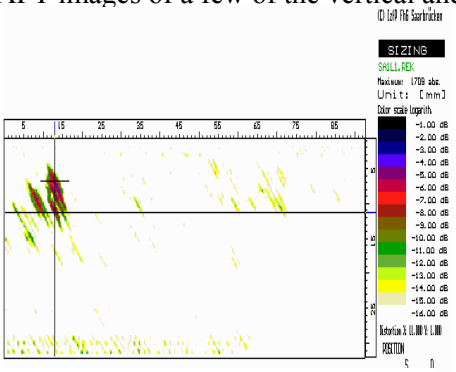

(a). Crack under Inconel cladding
Crack 1: 4.56mm

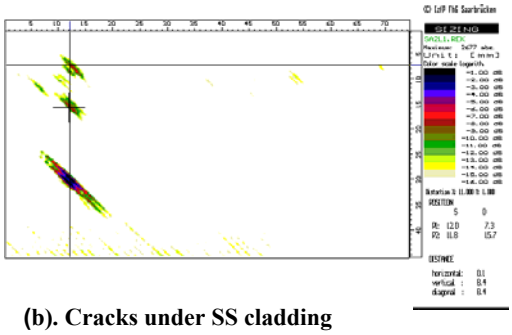

(b). Cracks under SS cladding
Crack 1: 8.4mm
Crack 2: 1.7mm

Figure 8 (a) and (b). SAFT images from vertical simulated cracks (slits)

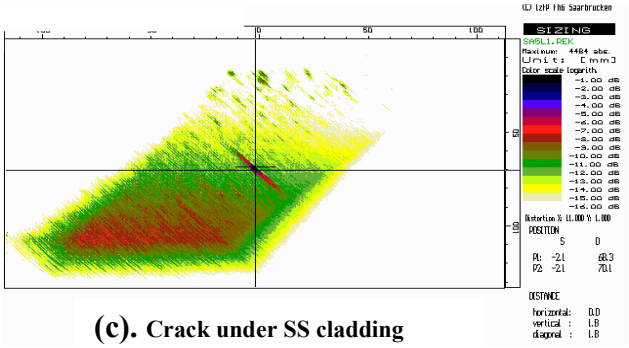

(c). Crack under SS cladding
Crack 2: 1.8mm

Figure 8(c). SAFT image from inclined simulated crack

The experimental results have shown excellent correlation between the actual and estimated through thickness height of the simulated cracks. In the case of vertical cracks, the sizing is obtained with accuracy of ±0.1 mm and in case of inclined cracks; accuracy is found to be ±0.31mm when ultrasonic SAFT is used. As it can be seen from the results, even the signals from the inclined cracks (10° and 15°) have sufficient S/N ratio due to SAFT processing. This is because of the fact that the technique does not directly depend upon the amplitude of the signal. Further, the problems encountered in TOFD with regard to sizing of near surface cracks were successfully overcome by SAFT, as detailed below:

TOFD technique suffers from a near surface effect caused by its inherent lateral wave. Difficulty is normally experienced to detect and size cracks starting from the interface between Inconel/stainless steel cladding and the ferritic base i.e. (5mm/6mm below the scanning surface). This is due to lateral wave, which obscures the tip-diffracted signals from the defects close to the surface and also due to the inherent lack of time resolution near the surface. The investigations revealed that the width (time duration) of the lateral wave for stainless steel and Inconel was 12mm and 18mm respectively. However, these cracks could be well detected and sized by scanning from the opposite surface of the blocks. Even the small crack of 1.9mm height could be detected as long as they are not influenced by the lateral wave. However the cracks less than 2mm height could be sized with an accuracy of

±0.7 to ±1mm only as against ±0.1 to ±0.2mm by SAFT. The SAFT could determine defects much close to scanning surface i.e. even up to 6mm. A typical image of a defect missed by TOFD is picked by SAFT distinctly in Block No.1 having Inconel clad of 5.4mm is shown in Figure 8(a). As more energy gets scattered in the clad due to coarse austenite structure resulting in the drop in the energy that enters the base material, the energy reflected from the crack would be less. This situation leads to lesser S/N ratio and reduces detection sensitivity. Even in such a situation inherent averaging in SAFT clearly enhances the detection sensitivity and the defect size can be accurately estimated. The detection of defects lying at greater depth below the top clad is further limited. As more divergence due to beam spread is also encountered. Hence conventional ultrasonic inspection is very much limited. Figure 8(b) shows a 1.88mm defect lying at a depth of 30.58mm from scanning surface. It can be shown that even a defect of such small dimension could be sized accurately. In addition to the clad and smaller size defects their inclination also seriously affects detection in cladded condition. Figure 8(c) shows a typical image of the defect embedded below stainless steel cladding having an inclined angle of 10° and crack height of 1.90mm. These studies demonstrate that it is possible to detect and characterize defects as small as 1.6mm height.

Conclusion: Experimental studies with the help of different artificial reflectors in different cladded specimens show that ultrasonic SAFT images can size defects with greater accuracy and with good S/N ratio. The near surface defect detection limited by the interference of lateral wave in TOFD could be overcome by SAFT. The study demonstrates that the SAFT can be applied to critical components where reliable and sensitive defect sizing is required.

Acknowledgements: Thanks are due to Council of Scientific & Industrial Research (CSIR), New Delhi, India for awarding the Senior Research Fellowship (SRF) to Ms. Sony Baby {Sanction No. 1(64) 010-2k2/1} and financially supporting her in the pursuance of her research study. We are thankful to the management of Bharat Heavy Electricals Limited, Tiruchirappalli and Indira Gandhi Centre for Atomic Research, Kalpakkam, India for providing necessary equipments and facilities for carrying out this experimental work. Thanks are also due to all the concerned officers / technical staff particularly Mr. P.S. Subbaraman, Sr.Scientific officer, NDTL/BHEL, Tiruchirappalli for extending the support for this study.

References:

1. Willy D, Kristensen, Erling Nielsen, Sven E. Iversen and Svend A Lund, SUPERsaft Ultrasonic Image Reconstruction, Non-Destructive Testing, Proceedings of 12th World Conference, 1989, 267-269.
2. Thomson, R N, A portable system for high resolution ultrasonic imaging on site, The British Institute of Non-Destructive Testing Conference, 21 September 1983, 281-285.
3. Busse, L J, Collins, H D and Doctor, S R, Review and discussion of the development of synthetic aperture focusing technique for ultrasonic testing (SAFT-UT), US Nuclear Regulatory commission Report NUREG/CR-3625, PNL-4957, March 1984.
4. Seydel, J, Ultrasonic Synthetic Aperture Focusing Techniques in NDT, Research Techniques in NDT (R.S. Sharpe), Academic Press, London, 6, 1982, 1- 47.
5. Stuart Kramer, Ultrasonic weld defect sizing using the Synthetic Aperture Focusing Technique, A review of progress in Quantitative Non-Destructive Evaluation, Plenum Press, New York, 8B, 1995-2002.
6. Schmitz, V, Muller, W and Schafer, G, Synthetic Aperture Focusing Technique: State of the art, Acoustical Imaging, 19, Edited by H. Ermert and H P Harjes, Plenum Press, New York, 1992, 545-551.
7. Pitkanen, J, Kauppinen, P, Jeskanen, H. and Schmitz, V, Evaluation of ultrasonic indications by using PC based Synthetic Aperture Focusing Technique (PCSAFT), NDTnet, January 1997, 02(01).
8. Sony Baby, Balasubramanian, T, Pardikar, R J, Palaniappan, M. and Subbaratnam, R, Time of Flight Diffraction (TOFD) technique for accurate sizing of embedded sub cladding cracks, Insight, September 2003, 45(9), 600-604.